# Mapping the coherence time of far-field speckle scattered by disordered media

**G. Soriano,*  M. Zerrad and C. Amra**

*Aix-Marseille Université, CNRS, Centrale Marseille,*
*Institut Fresnel, UMR 7249, 13013 Marseille, France*
**gabriel.soriano@fresnel.fr*

**Abstract:** The polarization and temporal coherence properties of light are altered by scattering events. In this paper, we follow a far-field approach, modelizing the scattering from disordered media with the scattering matrix formalism. The degree of polarization and coherence time of the scattered light are expressed with respect to the characteristics of the incident field.

© 2013 Optical Society of America

**OCIS codes:** (030.6600) Statistical optics; (030.1640) Coherence; (290.5855) Scattering, polarization; (030.6140) Speckle; (260.5430) Polarization; (290.5880) Scattering, rough surfaces; (290.7050) Turbid media.

---

## References and links

1. M. Zerrad, J. Sorrentini, G. Soriano, and C. Amra, "Gradual loss of polarization in light scattered from rough surfaces: Electromagnetic prediction," Opt. Express **18**, 15832–15843 (2010).
2. J. Sorrentini, M. Zerrad, G. Soriano, and C. Amra, "Enpolarization of light by scattering media," Opt. Express **19**, 21313–21320 (2011).
3. P. Réfrégier, M. Zerrad, and C. Amra, "Coherence and polarization properties in speckle of totally depolarized light scattered by totally depolarizing media," Opt. Lett. **37**, 2055–2057 (2012).
4. M. Zerrad, G. Soriano, A. Ghabbach, and C. Amra, "Light enpolarization by disordered media under partial polarized illumination: The role of cross-scattering coefficients," Opt. Express **21**, 2787–2794 (2013).
5. J. Goodman, *Statistical Optics* (Wiley-Interscience, 1985).
6. L. Mandel and E. Wolf, *Optical Coherence and Quantum Optics* (Cambridge University press, 1995).
7. E. Wolf, *Introduction to the Theory of Coherence and Polarization of Light* (Cambridge University Press, 2007).
8. G. Gbur and T. Visser, "The structure of partially coherent fields," Progress in optics **55**, 285 (2011).
9. T. Wang and D. Zhao, "Scattering theory of stochastic electromagnetic light waves," Opt. Lett. **35**, 2412–2414 (2010).
10. Z. Tong and O. Korotkova, "Theory of weak scattering of stochastic electromagnetic fields from deterministic and random media," Phys. Rev. A **82**, 033836 (2010).
11. C. Ding, Y. Cai, O. Korotkova, Y. Zhang and L. Pan, "Scattering-induced changes in the temporal coherence length and the pulse duration of a partially coherent plane-wave pulse," Opt. Lett. **36**, 517–519 (2011).
12. C. Ding, Y. Cai, Y. Zhang and L. Pan, "Scattering-induced changes in the degree of polarization of a stochastic electromagnetic plane-wave pulse," J. Opt. Soc. Am. A **29**, 1078–1090 (2012).
13. M. Salem, O. Korotkova, A. Dogariu, and E. Wolf, "Polarization changes in partially coherent electromagnetic beams propagating through turbulent atmosphere," Waves in Random Media **14**, 513–523 (2004).
14. J. Lancis, V. Torres-Company, E. Silvestre and P. Andrés, "Space-time analogy for partially coherent plane-wave-type pulses," Opt. Lett. **30**, 2973–2975 (2005).
15. H. Roychowdhury, G. P. Agrawal, and E. Wolf, "Changes in the spectrum, in the spectral degree of polarization, and in the spectral degree of coherence of a partially coherent beam propagating through a gradient-index fiber," J. Opt. Soc. Am. A **23**, 940–948 (2006).
16. W. Huang, S. Ponomarenko, M. Cada and G. P. Agrawal, "Polarization changes of partially coherent pulses propagating in optical fibers," J. Opt. Soc. Am. A **24**, 3063–3068 (2007).
17. J. Tervo, T. Setälä, and A. T. Friberg, "Theory of partially coherent electromagnetic fields in the space–frequency domain," J. Opt. Soc. Am. A **21**, 2205–2215 (2004).
18. P. Vahimaa and J. Tervo, "Unified measures for optical fields: degree of polarization and effective degree of coherence," Journal of Optics A: Pure and Applied Optics **6**, S41 (2004).

#194713 - $15.00 USD Received 26 Jul 2013; revised 5 Sep 2013; accepted 16 Sep 2013; published 2 Oct 2013

19. J. Ellis and A. Dogariu, "Complex degree of mutual polarization," Opt. Lett. **29**, 536–538 (2004).
20. P. Réfrégier and F. Goudail, "Invariant degrees of coherence of partially polarized light," Opt. Express **13**, 6051–6060 (2005).
21. P. Réfrégier and A. Roueff, "Intrinsic coherence: a new concept in polarization and coherence theory," Optics and photonics news **18**, 30–35 (2007).
22. J. G. Van Bladel, *Electromagnetic Fields* (Wiley-IEEE Press, 2007).
23. A. G. Voronovich, *Wave Scattering from Rough Surfaces* (Springer-Verlag, 1994).
24. J. Dainty, A. Ennos, M. Françon, J. Goodman, T. McKechnie, G. Parry, and J. Goodman, "Statistical properties of laser speckle patterns," Topics in Applied Physics **9**, 9–75 (1975).
25. J. Goodman, *Speckle Phenomena in Optics: Theory and Applications* (Roberts & Co, 2007).
26. W. H. Press, *Numerical Recipes in Fortran 77: the Art of Scientific Computing*, (Cambridge University Press, 1992).
27. J. Sorrentini, M. Zerrad, and C. Amra, "Statistical signatures of random media and their correlation to polarization properties," Opt. Lett. **34**, 2429–2431 (2009).

## 1. Introduction

It has been recently demonstrated how scattering from complex and disordered media – rough surfaces and inhomogenous bulks – can alter the polarization of light. When incident and scattered light are compared, decrease [1] as well as increase [2–4] of the so-called degree of polarization (DOP) can be met. Note that reported decreasing DOP comes from a spatial integration of the speckle, while increasing DOP, also called enpolarization, is a purely temporal feature. Those results, that mainly concern quasi-monochromatic fields, are now enriched with a study of the temporal coherence of scattered light.

The use of statistical concepts and methods is one of the cornerstones of modern Optics [5,6], and is ultimately tied to the quantized nature of light. It is now well established that space-time coherence of light is formalized at first-order in most generality with the coherence matrix and its spectral counterpart the Wolf's spectral density matrix [7, 8]. Such a theory was applied to weak scattering media under the Born approximation [9–12]. For example, turbulent atmosphere was addressed in [13]. Those derivations were based on a Green's function approach. Also, optical fibers were studied with the coherence matrix, this time under paraxial approximation [14–16]. In all cases, both temporal and spatial coherences were considered.

The paper is organized as follows. After this introduction, the DOP and coherence time are defined in section 2, with no reference to scattering. The electric field is here profitably modelized as a time-stationary process, since common detectors integrate the random fluctuations of light. For relating incident and scattered coherence matrices associated to a scattering event, our approach is based on the scattering matrix formalism rather than the Green's function, as detailed in section 3. Then, in section 4 we consider the case of an incident light with the self-correlations of its two modes proportional. This is a departure from generality that greatly simplifies and clarifies derivations. The expressions for the DOP and coherence time of the scattered light are given in section 5. They constitute the key point of this article. They rely on several integrals in the spectral domain. Those integrals are analytically tractable in the case of Gaussian self-correlation functions and Gaussian spectral degree of coherence. This case is detailed in section 6. In section 7 devoted to numerical illustration, the Gaussian case for incident light is coupled with the random phasors scattering model. This heuristic model, classically used in statistical Optics, is attached to the strongly scattering regime. Mappings of the scattered DOP and coherence time are shown, as well as distributions estimated from these mappings for these two quantities, in different configurations of incident light. The paper is finally concluded.

#194713 - $15.00 USD Received 26 Jul 2013; revised 5 Sep 2013; accepted 16 Sep 2013; published 2 Oct 2013
(C) 2013 OSA

## 2. Temporal coherence and polarization

In this paper, light is described by the two components of its time-stationary electric field in orthogonal directions. Far field regime is thus assumed, and dependency to spatial variables is discarded: spatial coherence will consequently not be addressed. The analytical signals of these components are denoted $E_x(t)$ and $E_y(t)$ and organized in a column vector:

$$\bar{E}(t) = \begin{bmatrix} E_x(t) \\ E_y(t) \end{bmatrix} \tag{1}$$

These components can easily be assumed to be centered variables: $\langle \bar{E}(t) \rangle = 0$ , with brackets denoting statistical mean.

The light is statistically characterized at first-order by the four self- and cross-correlation functions $\Gamma_{ij}(\tau) = \langle E_i^*(t) E_j(t+\tau) \rangle$, where asterisk is for the complex conjugation and $\tau$ the time lag. The coherence matrix is defined out of these four correlations and writes in matrix-vector notations:

$$\bar{\bar{\Gamma}}(\tau) = \langle \bar{E}^*(t) \bar{E}^{\mathrm{T}}(t+\tau) \rangle = \int_0^\infty \bar{\bar{W}}(\nu) e^{-2i\pi\nu\tau} d\nu \tag{2}$$

with $\bar{E}^{\mathrm{T}}$ the transpose of $\bar{E}$. The spectral density matrix, its Fourier transform, is denoted $\bar{\bar{W}}$ and is bounded to positive frequencies $\nu$ since $E_x(t)$ and $E_y(t)$ are analytical signals.

Both temporal coherence and polarization informations are encoded in the coherence matrix $\bar{\bar{\Gamma}}$ or its spectral counterpart $\bar{\bar{W}}$. Their coefficients do depend on the choice of the two orthogonal directions the electic field is projected on. The invariant quantities of the coherence matrix are its trace $T(\tau)$ and its determinant $D(\tau)$.

$$T = \Gamma_{xx} + \Gamma_{yy} \tag{3}$$

$$D = \Gamma_{xx}\Gamma_{yy} - \Gamma_{xy}\Gamma_{yx} \tag{4}$$

The so-called degree of polarization $P$ depends on both invariants, but only at time lag $\tau = 0$, while the so-called coherence time $\Delta\tau$ is built on the sole trace $T$ but for all time lags.

$$P = \sqrt{1 - \frac{4D(0)}{T(0)^2}} \tag{5}$$

$$\Delta\tau = \frac{1}{T(0)^2} \int_{-\infty}^{+\infty} |T(\tau)|^2 d\tau = \frac{\int_0^\infty \tilde{T}(\nu)^2 d\nu}{\left(\int_0^\infty \tilde{T}(\nu) d\nu\right)^2} \tag{6}$$

We will make use of the expression of the coherence time $\Delta\tau$ in the spectral domain, with $\tilde{T}(\nu) = \int_{-\infty}^{+\infty} T(\tau) e^{+2i\pi\nu\tau} d\tau$ the Fourier transform of the trace $T$.

Note that the definitions (5) and (6) are not unique. The so-called full width at half maximum is of common use for long, but appears quite unsuited to analytical derivations. The bandwidth $\Delta\nu$ of light is the spectral counterpart of the coherence time [6, § 4.3.3]. With Eq. (6) that can be met in [6, eq. 4.3-78 and 4.3-82], the coherence time-bandwidth product is a constant $\Delta\tau\Delta\nu = 1$. An increasing in coherence time is necessarily balanced by a decreasing in the bandwidth. Also exists [6, eq. 4.3-66] the more complex definition

$$\sqrt{\int \tau^2 |T(\tau)|^2 d\tau \Big/ \int |T(\tau)|^2 d\tau} \tag{7}$$

for the coherence time. Here, the product is only lower-bounded: $\Delta\tau\Delta\nu \geq 1/(4\pi)$, with possible variations of the coherence time at constant bandwidth. This reciprocity inequality can represent interesting physics, but the inequality turns to equality in the case of a Gaussian trace $T$. Since this paper ends in numerical results for the Gaussian case (sections 6 and 7), we stick from now on to Eq. (6) for the coherence time, that is both simple and analytically tractable.

The degree of polarization (5) and the coherence time (6) are respectively linked to the intensity contrast in interferometry and ellipsometry experiments. Recently, several alternative definitions of those quantities have been proposed in the literature [17–21], that takes into account other physical aspects of polarization and temporal coherence. These new results are left for future investigations.

## 3. Scattering matrix

The theory of electromagnetic wave scattering is generally formalized in time-harmonic regime. With the sole assumption that the scattering medium is linear, incident plane wave and scattered fields are linked by the so-called scattering matrix $\bar{\bar{\Sigma}}(\nu)$ [22, chap. 11] (see also [23]).

$$\bar{\mathscr{E}}_s(\nu) = \bar{\bar{\Sigma}}(\nu)\bar{\mathscr{E}}_i(\nu) \tag{8}$$

The incident field $\bar{\mathscr{E}}_i(t)$ is assumed to have a plane wave structure in the scattering region. With $\hat{\mathbf{r}}_\mathbf{i}$ the propagation direction, two independent components of the electric field in the polarization plane normal to $\hat{\mathbf{r}}_\mathbf{i}$ form the vector $\bar{\mathscr{E}}_i(t)$. The scattered field is detected in far field conditions. Discarding dependency to the distance between the scattering center and the detector, the scattered field is characterized by its scattering amplitude $\bar{\mathscr{E}}_s(t)$.

The scattering matrix completely characterizes the scattering medium at frequency $\nu$. This complex 2-matrix is a function of the incident and scattering directions $\hat{\mathbf{r}}_\mathbf{i}$ and $\hat{\mathbf{r}}_\mathbf{s}$. It writes:

$$\bar{\bar{\Sigma}} = \begin{bmatrix} \Sigma_{xx} & \Sigma_{xy} \\ \Sigma_{yx} & \Sigma_{yy} \end{bmatrix} \tag{9}$$

with $\Sigma_{xx}$ and $\Sigma_{yy}$ the co-polarized coefficients and $\Sigma_{xy}$ and $\Sigma_{yx}$ the cross-polarized coefficients. Remark that subscripts $x$ and $y$ denote different directions for incident and scattered fields.

The scattering matrix formalism can be extended to partially coherent and partially polarized incident light. With light considered as a random stationary process, the spectral density matrix is related to the generalized Fourier transforms of the fields by :

$$\langle \bar{\mathscr{E}}^*(\nu_1)\bar{\mathscr{E}}^\mathrm{T}(\nu_2)\rangle = \bar{\bar{W}}(\nu_2)\delta(\nu_2-\nu_1) \tag{10}$$

denoting $\delta$ the Dirac distribution. With (8) and in the case of a deterministic disordered medium, scattered and incident spectral density matrices become also directly connected :

$$\bar{\bar{W}}^s(\nu) = \bar{\bar{\Sigma}}^*(\nu)\bar{\bar{W}}^i(\nu)\bar{\bar{\Sigma}}^\mathrm{T}(\nu) \tag{11}$$

In many situations, including but not limited to quasi-monochromatic light, the variation of the scattering matrix over the incident light bandwidth can be neglected. We then write

$$\bar{\bar{\Gamma}}_s(\tau) = \bar{\bar{\Sigma}}^*(\nu_0)\bar{\bar{\Gamma}}_i(\tau)\bar{\bar{\Sigma}}^\mathrm{T}(\nu_0) \tag{12}$$

with $\nu_0$ the incident light central frequency. We can now focus on the determinant and trace, invariants of the scattered filed coherence matrix. With determinant property for matrix products, the determinant is simply:

$$D_s(\tau) = |D_\Sigma(\nu_0)|^2 D_i(\tau) \qquad D_\Sigma = \Sigma_{xx}\Sigma_{yy} - \Sigma_{xy}\Sigma_{yx} \tag{13}$$

that is proportional to the incident one. The expression of the scattered trace is less reducible:

$$T_s(\tau) = \mathrm{Tr}\left(\overline{\overline{M}}(\nu_0)\ \overline{\overline{\Gamma}}_i(\tau)\right) \qquad \overline{\overline{M}} = \overline{\overline{\Sigma}}^*\overline{\overline{\Sigma}}^\mathrm{T} = \begin{bmatrix} |\Sigma_{xx}|^2 + |\Sigma_{xy}|^2 & \Sigma_{xx}^*\Sigma_{yx} + \Sigma_{xy}^*\Sigma_{yy} \\ \left(\Sigma_{xx}^*\Sigma_{yx} + \Sigma_{xy}^*\Sigma_{yy}\right)^* & |\Sigma_{yx}|^2 + |\Sigma_{yy}|^2 \end{bmatrix} \quad (14)$$

with $\overline{\overline{M}}$ a positive hermitian matrix.

## 4. Incident field coherence matrix

To go further into the derivation, we focus on some specific incident light, that we define as follows. With central frequency $\nu_0$, the diagonal elements of its coherence matrix write

$$\begin{array}{ll} \Gamma_{xx}^i(\tau) = \Gamma_0\ e^{-2i\pi\nu_0\tau}\ g_i(\tau) & W_{xx}^i(\nu) = \Gamma_0\ \tilde{g}_i(\nu-\nu_0) \\ \Gamma_{yy}^i(\tau) = \beta_i\ \Gamma_0\ e^{-2i\pi\nu_0\tau}\ g_i(\tau) & W_{yy}^i(\nu) = \beta_i\ \Gamma_0\ \tilde{g}_i(\nu-\nu_0) \end{array} \quad (15)$$

where $g_i(\tau)$ is a real even function with $g_i(0) = 1$ and $\Gamma_0$ a real positive constant. The two self-correlation functions share the same shape $g_i(\tau)$, differing only in levels : real positive $\beta_i$ is the so-called polarization ratio. The two trivial examples for $g$ are the Gaussian function for Doppler-broadened sources and the exponential function for collision-broadened sources. Gaussian function is investigated in the next section. Following Eq. (6) in the spectral domain, the incident coherence time $\Delta\tau_i$ is ruled by function $g_i(\tau)$: with $T_i(0) = \Gamma_0(1+\beta_i)$,

$$\Delta\tau_i = \int_{-\infty}^{+\infty} |g_i(\tau)|^2 d\tau = \int_0^\infty \tilde{g}_i^2(\nu-\nu_0)d\nu \quad (16)$$

The incident cross-correlation function is more easily described in the spectral domain, introducing the so-called spectral degree of coherence $w_i(\nu)$:

$$W_{xy}^i(\nu) = (W_{yx}^i)^*(\nu) = \sqrt{\beta_i}\Gamma_0\tilde{g}_i(\nu-\nu_0)w_i(\nu) \qquad |w_i(\nu)| \leq 1 \quad (17)$$

Then determinant at null time lag writes

$$D_i(0) = \Gamma_0^2\beta_i(1-|\mu_i|^2) \qquad \mu_i = \frac{\Gamma_{xy}^i(0)}{\sqrt{\Gamma_{xx}^i(0)\Gamma_{yy}^i(0)}} = \int_0^\infty \tilde{g}_i(\nu-\nu_0)w_i(\nu)d\nu \quad (18)$$

leading to a classical formula for the incident DOP:

$$P_i = \sqrt{1 - \frac{4\beta_i}{(1+\beta_i)^2}(1-|\mu_i|^2)} \quad (19)$$

## 5. Scattered field temporal coherence and polarization

For the scattered field, the trace writes in the spectral domain

$$\tilde{T}_s(\nu) = \Gamma_0\chi\tilde{g}_i(\nu-\nu_0)(1+\Re e[\alpha w_i(\nu)]) \quad (20)$$

introducing for convenience

$$\chi = M_{xx}(\nu_0) + \beta_i M_{yy}(\nu_0) > 0 \qquad \alpha = \frac{2\sqrt{\beta_i}M_{yx}(\nu_0)}{\chi} \quad (21)$$

Note than $\chi$ vanishes only when the complete scattering matrix is zero, an uninteresting case that is discarded in this paper. With an intensity, that is the value of the trace at null time lag:

$$T_s(0) = \int_0^\infty \tilde{T}_s(\nu)d\nu = \Gamma_0\chi(1+\Re e[\alpha\mu_i]) \quad (22)$$

the scattered DOP is

$$P_s = \sqrt{1 - \frac{|D_\Sigma(\nu_0)|^2}{\chi^2} \frac{4\beta_i(1-|\mu_i|^2)}{(1+\Re e[\alpha\mu_i])^2}} \tag{23}$$

It is remarkable that the scattered DOP depends on the incident DOP through $\beta_i$ and $\mu_i$ and the scattering matrix through $\underline{\underline{M}}$, but not on the incident coherence time $\Delta\tau_i$. This property is not tied to incident fields with coherence matrix as detailed in section 4, and is most general for partially coherent and partially polarized light, as demonstrated in [4]. From Eq. (23) can be directly retrieved the sufficient condition for total repolarization of light, whatever the polarization of the incident light:

$$\Sigma_{xx}\Sigma_{yy} = \Sigma_{xy}\Sigma_{yx} \tag{24}$$

It is now time to estimate the numerator of coherence time (6) for the scattered field. This term

$$\int_0^\infty \tilde{T}_s^2(\nu)d\nu = \Gamma_0^2\chi^2\left(\Delta\tau_i + \frac{|\alpha|}{2}A + \Re e[2\alpha B + \frac{\alpha^2}{2}C]\right) \tag{25}$$

requires the evaluation of three new integrals, namely

$$A = \int_0^\infty \tilde{g}^2(\nu-\nu_0)|w(\nu)|^2 d\nu \tag{26}$$

$$B = \int_0^\infty \tilde{g}^2(\nu-\nu_0)w(\nu)d\nu \tag{27}$$

$$C = \int_0^\infty \tilde{g}^2(\nu-\nu_0)w^2(\nu)d\nu \tag{28}$$

Finally, the scattered field coherence time writes:

$$\Delta\tau_s = \frac{\Delta\tau_i + \frac{|\alpha|^2}{2}A + \Re e[2\alpha B + \frac{\alpha^2}{2}C]}{(1+\Re e[\alpha\mu_i])^2} \tag{29}$$

This time, the Eq. (29) relies the scattered trace to both incident coherence and polarization.

One can check that incident and scattered coherence times coincide at the limit $\alpha \to 0$. $\alpha$ is proportional to the term $M_{xy} = \Sigma_{xx}^*\Sigma_{yx} + \Sigma_{xy}^*\Sigma_{yy}$. There exist configurations where the cross-polarized coefficients $\Sigma_{yx}$ and $\Sigma_{xy}$ are negligible, such as rough surfaces with small heights compared to the central wavelength $\lambda_0 = c/\nu_0$, with $c$ the speed of light.

The same limiting value is reached in the totally polarized case when $w(\nu) = \mu_i = e^{i\varphi_0}$. In that case, the integrals analytically write $A = \Delta\tau_i$, $B = \mu_i\Delta\tau_i$ and $C = \mu_i^2\Delta\tau_i$. Equal scattered and incident coherence times should also be met at the limit $\mu_i \to 0$, so that other defining conditions on the spectral degree of coherence, along with Eqs. (17)-(18), are that integrals $A$, $B$ and $C$ tend toward zero when $\mu_i$ vanishes. These conditions are implemented in the following section.

## 6. The Gaussian case

The function $g_i(\tau)$ in the self-correlation terms is choosen real Gaussian, with only one real positive parameter, the incident coherence time $\Delta\tau_i$.

$$g_i(\tau) = e^{-\frac{\pi}{2}\left(\frac{\tau}{\Delta\tau_i}\right)^2} \quad w(\nu+\nu_0) = e^{i\varphi_0}e^{-2\pi(z\nu)^2} \tag{30}$$

The spectral degree of coherence is also Gaussian, but complex, with complex parameter $z = re^{i\theta}$. A third real parameter, the constant phase $\varphi_0$, is added. With a central frequency

#194713 - $15.00 USD Received 26 Jul 2013; revised 5 Sep 2013; accepted 16 Sep 2013; published 2 Oct 2013
(C) 2013 OSA

$\nu_0$ sufficiently large compared to the bandwith $\Delta\nu_i = 1/\Delta\tau_i$, the bounds of integrals in Eq. (16), Eq. (18) and Eqs. (26)-(28) can be extended to the whole real axis. All those integrals are thus analytical, with expressions:

$$\begin{array}{ll} \mu_i = \frac{e^{i\varphi_0}}{\sqrt{1+\left(\frac{z}{\Delta\tau_i}\right)^2}} & A = \frac{\Delta\tau_i}{\sqrt{1+\Re e\left[\left(\frac{z}{\Delta\tau_i}\right)^2\right]}} \\ B = \frac{\Delta\tau_i e^{i\varphi_0}}{\sqrt{1+\frac{1}{2}\left(\frac{z}{\Delta\tau_i}\right)^2}} & C = \frac{\Delta\tau_i e^{2i\varphi_0}}{\sqrt{1+\left(\frac{z}{\Delta\tau_i}\right)^2}} \end{array} \tag{31}$$

## 7. Numerical simulations with the random phasors scattering model

We consider a strongly scattering medium, such as an inhomogeneous bulk with high optical index variations or a rough surface with steep slopes or peak to valley heights larger than the central wavelength. Such a medium is easily modelized with the random phasors sum phenomenological model [24, 25]. In accordance with this model, each of the four coefficients of the scattering matrix (9) is modelized by the far field scattered by $n^2$ random phasors placed on a plane square regular grid with mesh size $\delta_x$. Those phasors are circular complex gaussian random variables of zero mean and equal variance. They are statistically independent, but the scattered field is obtained by interference of their individual fields. The computation is efficiently performed with two-dimensional Fast Fourier Transforms (FFT) on $N = np$ points along each dimension, using zero-padding [26]. With $\theta$ the polar angle and $\varphi$ the azimuthal angle, scattering directions can be pointed by the two horizontal components of the wavevector

$$\left\{ \begin{array}{l} k_x = (\omega_0/c)\sin\theta\cos\varphi \\ k_y = (\omega_0/c)\sin\theta\sin\varphi \end{array} \right. . \tag{32}$$

The scattered field is estimated on a regular grid in the $(k_x, k_y)$ plane with a mesh size $\delta_k = \frac{2\pi}{N\delta_x}$. Each direction $(k_x = i\delta_k, k_y = j\delta_k)$ on this grid is parametered by two integer numbers $(i, j)$ in the range $[1-N/2 : N/2]$, and corresponds to a pixel on the maps of forthcoming figures. The covered region includes $n^2$ speckle grains, with $p^2$ pixels per grain. Those directions are paraxial under condition $\delta_x \ll \lambda_0 = \frac{2\pi c}{\omega_0}$ that is assumed thereafter.

The real part of $z^2$ should be positive, in order for $w(\nu)$ to remain a bounded function of the frequency. This leads to the following inequality:

$$|\varphi_0 - \arg\mu_i - k\pi| \leq \frac{1}{2}\arccos(|\mu_i|^2) \tag{33}$$

with $k$ an integer. At the limit of the totally depolarized incident light, the modulus $r$ of the complex parameter $z$ tends toward infinity. In order to avoid infinitely dense oscillations of the spectral degree of coherence $w(\nu)$, $z$ is forced to be real at this limit.

$$\mu_i \to 0 \qquad r \to \infty \qquad \theta \to 0 \tag{34}$$

A single realization of the scattered field is estimated using the previously described model with numbers $n = 64$ and $p = 32$. The intensity $T_S(0)$ with Eq. (22), the DOP with Eq. (23) and the coherence time with Eq. (29) are computed for all pixels and a set of values for parameters $\beta_i$, $\mu_i$ and $z = r\,e^{i\theta}$ of the incident field correlation matrix.

A complete example is illustrated on Fig. 1 for parameters $\beta_i = 1$, $\mu_i = 1/2$, $\theta = \pi/8$ and $r \simeq 1.8$. All maps are restricted to the $1 \leq i, j \leq 512$ region for clarity. Nevertheless, the probability density functions of those three quantities are estimated over the full $N^2$ points, that is a statistical sample of around four million values. The intensity is normalized by its mean value,

#194713 - $15.00 USD Received 26 Jul 2013; revised 5 Sep 2013; accepted 16 Sep 2013; published 2 Oct 2013
(C) 2013 OSA

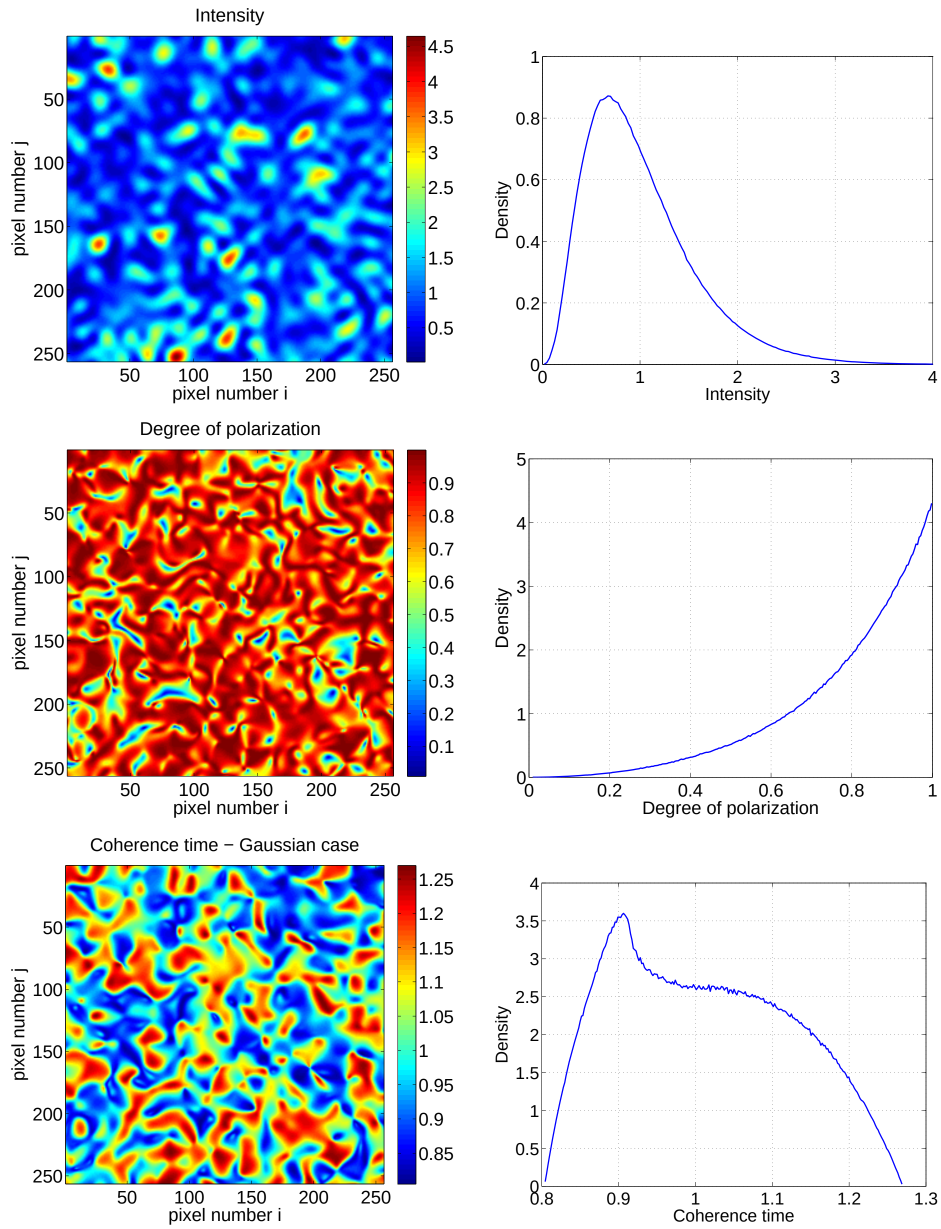


Fig. 1. Maps (left column) and densities (right column) of the scattered normalized intensity (top line), degree of polarization (middle line) and coherence time (bottom line) for parameters $\beta = 1$, $\mu_i = 1/2$, $\theta = \pi/8$ and $r \simeq 1.8$.

and the scattered field coherence time is normalized by the incident field coherence time. This kind of figures has already been published in [27] for the intensity and in [4] for the degree of polarization, although a different theoretical approach was undergone. They are given for consistency: the gamma law of order 4 is notably retrieved for the intensity. On the contrary, the coherence time maps and densities are novel. The coherence time map share the same granular structure as the degree of polarization, with variations at the scale of the speckle grain. Even if the most probable value is $0.9\Delta\tau_i$, the distribution is centered on the incident coherence time. Its coefficient of variation, that is the standard deviation to mean ratio, is around 11% in this case.

On Fig. 2, the polarization ratio $\beta_i$ is varied. Here again, as for all numerical simulations in the section, the mean scattered coherence time matches the incident coherence time. It appears that the scattered coherence time has a coefficient of variation that slightly reduces when the polarization ration departs from unity. Note that in the strongly scattering regime, a value of $\beta_i$ and its inverse share the same DOP and coherence time densities.

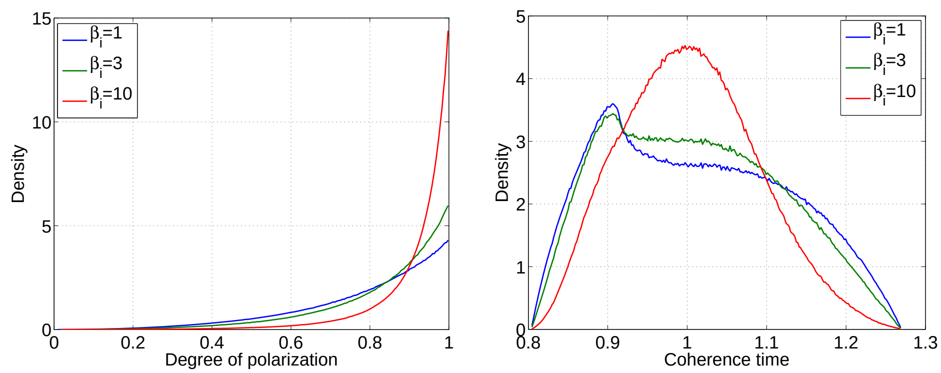


Fig. 2. Densities of the degree of polarization (left) and coherence time (right) for parameters $\mu_i = 1/2$, $\theta = \pi/8$, $r \simeq 1.8$ and three values of parameter $\beta_i$.

From now on, the polarization ratio is fixed to unity, and the cross-correlation coefficient is varied from zero to one. In this study, Eqs. (33)-(34) are conditions enforced by setting:

$$\theta = \frac{\pi}{4}\mu_i \tag{35}$$

The variations of the coherence time coefficient of variation and the mean DOP are reported on Fig. 3, with several examples of coherence time densities. It can be noted how these last densities tend toward the Dirac distribution coinciding with the incident coherence time at both limits $\mu_i \to 0$ and totally polarized light $\mu_i \to 1$. In the given configuration, the coherence time coefficient of variation reaches its maximum value 13.5% at $\mu_i = 0.8$.

## 8. Conclusion

It is shown in this paper that the scattering matrix formalism is well-fitted for the modelization of the polarization and temporal coherence properties of light altered by scattering from disordered but deterministic media. The main outcome is that the coherence time of scattered light depends on the scattering matrix of the disordered media and both the DOP and the temporal coherence of the incident light, while the scattered DOP is independent of the incident coherence time. This result has been derived under the assumption that the scattering matrix has

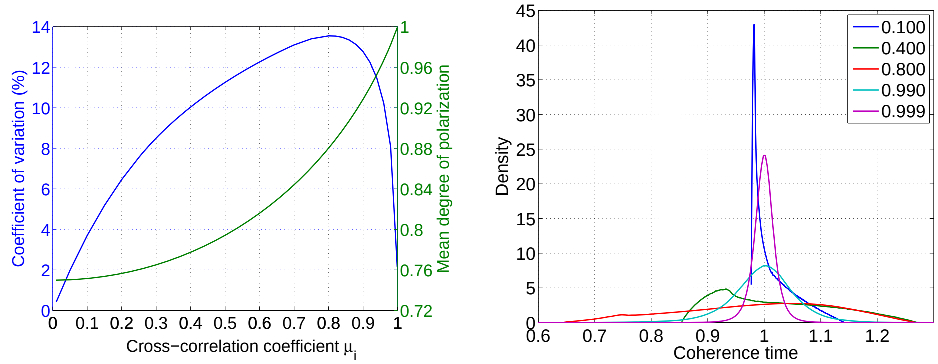


Fig. 3. The coherence time coefficient of variation and the mean DOP against the cross-correlation coefficient (left) and densities of the coherence time for several values of the cross-correlation coefficient (right) for parameters $\beta_i = 1$ and $\theta = \frac{\pi}{4}\mu_i$.

negligible spectral variation over the incident light bandwidth. The exact domain of validity of such an assumption, that includes the quasi-monochromatic regime, remains to state.

It appears that the estimation of the scattered field coherence time requires the computation of several integrals that involves the elements of the incident field spectral density matrix. In the simplifying case where the diagonal elements of this matrix are proportional, the number of integral is three. Moreover, those integrals are analytical for Gaussian functions. The scattered field DOP and coherence time can thus easily be mapped in strongly scattering regime, with the random phasors model. Influence of the incident polarization parameters on the scattered field coherence time is illustrated. In all our numerical examples, scattered coherence time distribution is centered on the incident coherence time, with standard deviation up to 13.5%. We have checked that this deviation vanishes at both limits of totally polarized and depolarized incident light.

Such a study can be continued or extended in many ways. We briefly mention three of them. First, Gaussian correlation functions correspond to Doppler-broadened sources of light, but the exponential correlation functions case is also interesting and commonly met. Here, the integrals can be estimated numerically. Second, for light with large spectral bandwidth, the nondispersive scattering matrix asumption no longer hold. In this case, a more physical scattering model is required, as the random phasor model cannot predict relevant spectral variations. Third, the theory can be generalized to incident field matrix with arbitrary diagonal elements, since common sources such as Gaussian Schell model frequently exhibit disproportional diagonal elements.

## Acknowledgments

This work was performed in the TraMEL project thanks to the financial support of French National Research Agency (Project TraMEL # 10-BLAN-0315).